HHS Public Access

Author manuscript

Cancer Discov. Author manuscript; available in PMC 2019 January 22.

Published in final edited form as:

Cancer Discov. 2018 March ; 8(3): 288–303. doi:10.1158/2159-8290.CD-16-1406.

An RNA-based digital circulating tumor cell signature is predictive of drug response and early dissemination in prostate cancer

David T. Miyamoto[1,3,*], **Richard J. Lee**[1,4,*], **Mark Kalinich**[1], **Joseph LiCausi**[1], **Yu Zheng**[1], **Tianqi Chen**[8], **John D. Milner**[1], **Erin Emmons**[1], **Uyen Ho**[1], **Katherine Broderick**[1], **Erin Silva**[1], **Sarah Javaid**[1], **Tanya Todorova Kwan**[1], **Xin Hong**[1], **Douglas M. Dahl**[1,6], **Francis J. McGovern**[1,6], **Jason A. Efstathiou**[1,3], **Matthew R. Smith**[1,4], **Lecia V. Sequist**[1,4], **Ravi Kapur**[1], **Chin-Lee Wu**[1,7], **Shannon L. Stott**[1,2,4], **David T. Ting**[1,4], **Anita Giobbie-Hurder**[8], **Mehmet Toner**[2,5], **Shyamala Maheswaran**[1,5,**], and **Daniel A. Haber**[1,4,9,**]

[1]Massachusetts General Hospital Cancer Center, Harvard Medical School, Charlestown, MA 02129

[2]Center for Bioengineering in Medicine, Harvard Medical School, Charlestown, MA 02129

[3]Department of Radiation Oncology, Harvard Medical School, Charlestown, MA 02129

[4]Department of Medicine, Harvard Medical School, Charlestown, MA 02129

[5]Department of Surgery, Harvard Medical School, Charlestown, MA 02129

[6]Department of Urology, Harvard Medical School, Charlestown, MA 02129

[7]Department of Pathology, Harvard Medical School, Charlestown, MA 02129

[8]Dana Farber Cancer Institute, Harvard Medical School, Boston, MA 02115

[9]Howard Hughes Medical Institute, Chevy Chase, MD 20815

Abstract

Blood-based biomarkers are critical in metastatic prostate cancer, where characteristic bone metastases are not readily sampled, and they may enable risk stratification in localized disease. We established a sensitive and high-throughput strategy for analyzing prostate circulating tumor cells (CTCs) using microfluidic cell enrichment followed by digital quantitation of prostate-derived transcripts. In a prospective study of 27 metastatic castration-resistant prostate cancer patients treated with first-line abiraterone, pretreatment elevation of the digital CTC_M Score identifies a high risk population with poor overall survival (HR 6.0, P=0.01) and short radiographic progression-free survival (HR 3.2, P=0.046). Expression of *HOXB13* in CTCs identifies 6/6 patients with ≤12 months survival, with a subset also expressing the *AR-V7* splice variant. In a second cohort of 34 men with localized prostate cancer, an elevated preoperative CTC_L Score

**Corresponding authors: Dr. Daniel Haber and Dr. Shyamala Maheswaran, Massachusetts General Hospital, Bldg 149, 13th Street, Charlestown, MA 02129, dhaber@mgh.harvard.edu and maheswaran@helix.mgh.harvard.edu.

*Denotes equal contribution

Conflict of Interest Statement: D.A.H., S.M., and R.J.L. have received sponsored research support from Janssen. D.A.H. is on the Scientific Advisory Board for Janssen.

predicts microscopic dissemination to seminal vesicles and/or lymph nodes (P<0.001). Thus, digital quantitation of CTC-specific transcripts enables noninvasive monitoring that may guide treatment selection in both metastatic and localized prostate cancer.

Keywords

CTCs; prostate cancer; abiraterone; digital PCR; AR-V7

Introduction

The application of blood-based biomarkers is emerging as an important strategy for individualizing therapeutic choices in prostate cancer in the settings of both metastatic and localized disease. In advanced prostate cancer, typically characterized by bone metastases that cannot be readily biopsied for tumor sampling (1), multiple increasingly potent therapeutic regimens have been recently approved, resulting in a pressing need for noninvasive tumor-specific predictors of response (2, 3). In virtually all cases, metastatic prostate cancer initially responds to androgen deprivation therapy (ADT), which suppresses the primary driver of proliferation in this tissue. Responses, however, are limited in duration and the development of metastatic castration-resistant prostate cancer (mCRPC) necessitates the application of alternative therapies, including potent suppressors of androgen synthesis (e.g. abiraterone), inhibitors of the androgen receptor (AR) itself (e.g. enzalutamide), vaccine therapy (sipuleucel-T), cytotoxic chemotherapy (docetaxel or cabazitaxel), bone-tropic radioisotopes such as Radium-223, and PARP inhibitors (4, 5). In this context, CTC quantitation has been proposed as a potential surrogate endpoint to facilitate the selection of treatment algorithms (6), although the small number of cells identified visually in blood specimens from patients with prostate cancer and the lack of specific molecular determinants of response have limited its clinical utility (7).

To date, most molecular alterations in prostate cancer that have potential therapeutic implications have been centered around the *AR* gene itself, including gene amplification or overexpression, activating mutations, or alterations in transcriptional co-activators (8). Measuring AR signaling output through expression ratios of androgen-induced versus androgen-repressed transcriptional targets has been proposed as an integrated readout for these complex AR pathway alterations (9). Multiple *AR* gene splicing variants encoding aberrant ligand-independent transcriptional activators have also been described in mCRPC (10). These AR isoforms are rarely expressed in primary prostate cancer, but they are readily detected in mCRPC, with single cell RNA sequencing of CTCs identifying multiple variants within different tumor cells from the same patient and even within individual CTCs (11). One of the most common variants, AR-V7, is noteworthy in that it encodes a novel cryptic exon, CE3, which may be detected using either CE3 exon-specific RNA-based PCR amplification or CE3 exon-targeted immunohistochemical staining. In patients with mCRPC receiving AR-targeting therapies, detection of AR-V7 in CTCs has been correlated with a poor outcome (12–14). In addition to alterations in AR signaling, additional pathways have been implicated in the progression towards androgen-independent disease, including

expression of the glucocorticoid receptor (GR) (15), activation of the non-canonical Wnt pathway (11), and evolution of tumor cells toward a neuroendocrine phenotype (16).

In contrast to mCRPC, early stage localized prostate cancer is often characterized by good prostate-cancer specific outcomes regardless of treatment modality, including radical prostatectomy, radiation therapy, or active surveillance (17). However, a subset of patients are at high risk of tumor dissemination outside of the prostate gland, most often to the seminal vesicles and pelvic lymph nodes, and eventually to bone. Standard clinicopathologic parameters including Gleason score, serum PSA, and clinical T-stage (18, 19) and clinical nomograms (20, 21) provide estimates for risk stratification, but they rely primarily on pathologic assessment of prostate core biopsies, which are subject to undersampling errors and often underestimate the true pathologic stage of the cancer (22, 23). Interestingly, CTCs have been detected in the blood of a fraction of men with localized prostate cancer, which are cleared within 24 hours of surgical resection of the prostate, although the clinical significance of these findings has not been established (24–26).

While CTCs provide a source of tumor material for serial, noninvasive sampling of prostate cancer, their broad application in clinical monitoring has been precluded by technological hurdles, including complex platforms for rare cell isolation from blood samples and sophisticated cell-based imaging and scoring. Recently, the development of microfluidic technologies has allowed efficient processing of blood specimens for CTC capture, including efficient depletion of hematopoietic cells to enable tumor-epitope independent enrichment of untagged CTCs (27). However, the reliance on microscopic imaging and quantitation of immunofluorescence-based signals in enriched but impure CTC populations remains a critical limitation. We recently demonstrated, using single cell RNA sequencing of prostate CTCs isolatedby negative depletion microfluidics, that these microfluidically isolated circulating cancer cells contain highly intact RNA, readily distinguishable from that of contaminating leukocytes in the CTC-iChip output, thereby enabling RNA-based diagnostics (11). Assessment of CTC RNA molecular signatures using a droplet digital PCR assay enables rapid and reliable detection of CTCs in hepatocellular carcinoma, and may allow for early detection of liver cancers (28). Here, we established an RNA-based molecular signature that allows high throughput and highly quantitative detection of prostate CTCs following microfluidic enrichment. Ina prospective trial of men with mCRPC treated with first-line abiraterone, we identify predictive CTC-derived molecular markers of clinical outcome. Furthermore, in men with clinically localized prostate cancer undergoing radical prostatectomy, digital detection of CTCs is predictive of pathologic seminal vesicle invasion and lymph node dissemination identified at the time of surgery.

Results

Generation of CTC digital signature using prostate-lineage transcripts

Given the well recognized limitations inherent in fluorescence-based imaging and scoring of CTCs admixed with contaminating blood cells, we tested whether RNA-based digital PCR quantitation could provide a higher throughput, more sensitive and more specific readout of prostate CTCs. We recently established such an assay for detection of liver-derived CTCs in patients with hepatocellular carcinoma (28), and we reasoned that prostate-derived CTCs

may also express specific transcripts that are unique to this tissue of origin and are undetectable in normal blood cells, even using a highly sensitive digital PCR assay (Suppl. Fig. S1A). Microfluidic (CTC-iChip) depletion of hematopoietic cells from blood samples achieves 10^4 to 10^5 purification of CTCs, with approximately 500 WBCs remaining per 1mL of initially processed whole blood (27). The high quality of RNA within the purified CTCs allows the application of digital droplet-PCR, in which rare cDNA templates are encapsulated within lipid droplets, followed by PCR amplification and fluorescence scoring of positive droplets (29). The combination of initial microfluidic whole cell enrichment of CTCs from blood, followed by RNA-based digital PCR of CTC-derived transcripts, thus allows exceptionally high-sensitivity scoring of prostate cancer cells that have invaded into the bloodstream.

To test the application of this strategy for prostate CTC detection, we first identified a panel of prostate-specific transcripts whose expression is virtually absent in normal hematopoietic cells, even using highly sensitive droplet digital PCR detection. We selected multiple markers, both to address the known heterogeneity of prostate cancer cells, as well as to allow interrogation of cellular signaling pathways, including AR activity. We derived an initial set of 40 candidate genes, both from RNA sequencing of single prostate CTCs (11), as well as from publicly available expression databases (Suppl. Fig. S1B; Suppl. Table S1). Eleven transcripts were identified as having high levels of expression in prostate tissue and/or prostate cancer, but without detectable RNA reads in normal blood cells contaminating the microfluidic CTC-iChip product (Suppl. Fig. S1B). Multiple primers and conditions were optimized for a set of 8 genes, which together provided the most robust signal in rare prostate cancer cells admixed with normal blood cells. To initially confirm differential expression of the selected genes, we used single cell RNA sequencing of CTCs individually isolated from patients with metastatic prostate cancer, compared with RNA seq of single leukocytes contaminating the microfluidic CTC-iChip product. Indeed, single cell RNA-Sequencing reads for these transcripts within 76 CTCs from 12 patients with metastatic prostate cancer show massive enrichment, compared with matched single leukocytes (Fig. 1A; RNA-seq data from (11) and GEO GSE67980). These genes include androgen responsive transcripts KLK3 (PSA), KLK2, TMPRSS2, and AGR2; androgen-repressed transcripts FOLH1 (PSMA) and HOXB13; and androgen-independent transcripts FAT1 and STEAP2. To avoid dilution of rare templates while enabling amplification of multiple markers, we designed a multiplex assay (2 reactions with 4 genes per reaction), with differing relative ratios of FAM and HEX fluorescence to define the identity of the amplified product (Fig.1B; Suppl. Fig. S1C). A multi-class support vector machine (SVM) classifier algorithm was developed to automatically classify droplets according to their position on the FAM-HEX coordinate system (Fig.1D; see Methods).

To validate the assay, we first micromanipulated individual cells of the prostate cancer line LNCaP, and introduced these into 4 mL aliquots of whole blood from healthy donors, followed by processing through the CTC-iChip and droplet digital PCR quantitation. Introduction of a single LNCaP cell into a control blood sample generated 150 positive droplets (SD = 65.3), with a progressive increase in signal as 3, 5,10, and 50 cells were spiked into the blood samples (5562 ± 1853 droplets for 50 prostate cell input) (Fig. 1C).

The distribution of signal among the 8 prostate- lineage transcripts remained comparable with increasing numbers of LNCaP cell input (Suppl. Fig. S1D).

CTC scoring in patients with metastatic prostate cancer

We tested the digital CTC detection strategy in 12 patients with metastatic prostate cancer, compared with 8 patients with localized prostate cancer, 34 male healthy blood donors (19 were >50 years old; 15 were <50 years old), and 5 female controls (see Suppl. Table S2 for clinical details). The observed signal across all 8 markers is shown in Fig. 2A. Using the 12 patients with metastatic prostate cancer (median age 67 years) and the 19 age-matched male controls (all age >50 years; median age 63 years), we examined the signal-to-noise ratio for each of the 8 genes and derived a digital CTC score by weighing each of these in proportion to the median difference between mCRPC patients and age matched controls (Fig. 2B; Suppl. Fig. S2; see Methods). We identified this measurement as CTC_M Score (for metastatic). A positive CTC_M Score was present in 11/12 (92%) patients with metastatic prostate cancer, compared with 0/34 healthy male blood donors (P=0.008). Under these stringent criteria, none of the 12 patients with localized prostate cancer had detectable CTC_M Scores. Interestingly, while we established scoring criteria for highest specificity in monitoring patients with metastatic prostate cancer, low level digital signal in several genes was present in some individuals with localized cancer (Fig. 2A). Among healthy individuals, very low level signal was present, primarily in androgen-independent transcripts, such as the embryonic cadherin FAT1, with females and men older than age 50 having higher background signal than men younger than age 50.

Across patients with mCRPC, the total digital CTC_M Score signal was not significantly correlated with serum PSA protein measurements (R^2=0.03; P=0.58) (Fig. 2D), a finding that is consistent with prior observations that visual immunofluorescence-based enumeration of CTCs is not well correlated well with serum PSA across different patients (24). The levels of serum PSA were only slightly better correlated with the quantitation of CTC-derived *KLK3* (PSA) mRNA (R^2=0.36; P=0.04) (Fig. 2E). Taken together, these observations indicate that, by integrating multiple AR-dependent and independent transcripts within invasive tumor cells in the blood, the digital CTC_M Score provide information on disease status that is non-overlapping and potentially orthogonal to serum PSA measurements.

Detection of AR-V7 and TMPRSS2-ERG prostate cancer-specific transcripts in CTCs

While recurrent missense mutations are rare in prostate cancer, two specific RNA fusion transcripts are characteristic of this tumor type. To complement the quantitation of prostate lineage-based transcripts in CTCs, we developed droplet PCR assays for both the *TMPRSS2-ERG* fusion transcript, which is present in about half of prostate cancer cases (30), and the *AR-V7* mRNA splice variant, which constitutes a marker of resistance to AR-targeted therapies (12). Both tests were highly specific and sensitive when applied to individual prostate cancer cells spiked into control whole blood specimens, followed by CTC-iChip purification (Fig. 3A). When applied to blood samples from men with metastatic prostate cancer, 5 of 15 (33%) mCRPC patients had the *TMPRSS2-ERG* translocation, 8 (53%) had the *AR-V7* splice variant, and 4 (27%) had both cancer-associated transcripts in their CTCs (Fig. 3B). Blood samples from 12 age-matched healthy male donors were

negative for both transcripts (Fig. 3B). As expected, men whose CTCs were positive for *TMPRSS2-ERG* had archival primary tumors that were largely concordant for that marker, as assessed by droplet digital PCR (Fig. 3C). In contrast, presence of AR-V7 was discordant between primary prostate cancers (1/15) and matched CTCs subsequently isolated from these patients in the setting of metastatic disease (8/15) (Fig. 3C), consistent with its characterization as a marker that emerges in the setting of treatment for advanced refractory mCRPC (31).

Prospective monitoring of patients on first-line abiraterone therapy.

Virtually all patients with metastatic prostate cancer experience an initial clinical response to androgen deprivation therapy (ADT), but subsequent treatments are marked by considerable heterogeneity. As tumors develop castration-resistance, about half of patients have a sustained response to treatment with the potent androgen synthesis inhibitor abiraterone, while others have only a short response and would hence potentially benefit from other treatments or combination therapies (32). To test whether CTC-derived signatures provide predictive markers of response to AR-targeted therapies after ADT, we prospectively evaluated 27 patients with mCRPC who were initiating abiraterone therapy in the first-line setting (Suppl. Table S3).

We applied the RNA-based prostate CTC_M Score, *AR-V7*, and *TMPRSS2:ERG* assays to microfluidically enriched CTCs at the baseline pretreatment time point (Fig. 4A). To compare the digital CTC assay with more traditional immunofluorescence-based detection of CTCs, each blood sample was processed through the CTC-iChip and the output was equally divided between immunofluorescence-based microscopy scoring for protein expression of EpCAM, CK8, CK18, CK19, PSA, and PSMA, in comparison to the digital CTC assay (Fig. 4A). As expected, concordance between microscopic scoring and digital readouts was evident in samples with high numbers of CTCs, but the digital-CTC assay was far more sensitive in identifying cases below microscopic detection, even using sophisticated multispectral fluorescence-based imaging (R^2=0.01; P=0.6; Fig. 4B). A poor correlation between serum PSA and digital-CTC score was also noted in this cohort (R^2=0.16; P=0.049; Suppl. Fig. S3A and S3B).

With a median follow-up time of 13 months among alive patients, an elevated CTC_M Score was significantly predictive of worse overall survival (Fig. 4C; HR 6.0, P=0.01) and rapid radiographic progression after abiraterone in the first line setting (Fig.4D; HR 3.2, P=0.046). Similar results were obtained using immunofluorescence microscopy-based CTC enumeration (Suppl. Fig. S3C and S3D), confirming the known correlation between CTC enumeration and prognosis in metastatic prostate cancer (33). Of the genes that comprise the CTC_M Score, expression of the AR-regulated genes *HOXB13, FOLH1, KLK2, KLK3*, and *AGR2* were each individually significantly predictive of lower overall survival (Suppl. Fig. S3E) and almost all of these AR-regulated genes were also predictive for worse radiographic progressionfree survival (Suppl. Fig. S3F). In particular, expression within CTCs of *HOXB13*, a gene associated with aberrant AR signaling and with more aggressive hormone refractory prostate cancer, was significantly correlated with worse overall survival (Fig. 4E;

HR 11.8, P=0.004; median 12 months vs. not reached), as well as radiographic progression (Suppl. Fig. S4A; HR 3.9, P=0.011; median 5 months vs. not reached).

Expression of the *AR-V7* mRNA splice variant has been detected in patients with mCRPC, where it has been shown to predict resistance to abiraterone and enzalutamide (12–14). Applying the digital CTC assay to patients in this prospective study of first-line abiraterone, quantitative measurement of *AR-V7* in pre-treatment blood samples revealed a range of 0 to 220 transcripts per mL blood (median =1.0). *AR-V7* expression was detectable at a level higher than 2 standard deviations above the mean signal in healthy donors in 4/22 (18%) patients at the pre-treatment time point. In this setting, the presence of a high level of *AR-V7* in CTCs was predictive of shorter overall survival (Fig. 4F) and radiographic progression-free survival (Suppl. Fig. S4B), particularly at a threshold greater than 14.7 transcripts per mL (see Methods). In contrast to *AR-V7*, the presence of *TMPRSS2-ERG* translocation in CTCs was not predictive of clinical outcome (Suppl. Figs. S4C and S3D).

To examine the predictive value of combining pre-treatment detection of CTC-derived markers *HOXB13* and *AR-V7* in identifying patients at high risk of early death (<12 months) following first-line abiraterone, we examined these two markers in the 22 mCRPC patients who had been tested for both (Fig. 4G). Of 6 patients who had early death on first-line abiraterone, all 6 were positive for *HOXB13* expression, while only 2 had an elevated level of *AR-V7* (Fig. 4G and Suppl. Fig. S4F), 6/13 (46%) of men with HOXB13-positive signal had early death, compared with 0/14 (0%) of patients without *HOXB13* expression in CTCs (Fig. S4E; P = 0.006). Thus, while *AR-V7* expression above the digital threshold of 14.7 transcripts per mL blood is highly specific for prediction of progression on first-line abiraterone, *HOXB13* expression identifies additional non-responding patients, in whom suppression of androgen production is insufficient to achieve a sustained tumor response.

CTC signatures in patients with localized prostate cancer.

Given the potential utility of the CTC Score in guiding therapy for metastatic prostate cancer, we explored whether a similar analysis may also be informative in the setting of localized prostate cancer. Compared with metastatic prostate cancer, fewer men with localized prostate cancer have detectable CTCs using traditional CTC imaging analyses, and the number of CTCs per ml of blood is considerably lower (24–26, 34). We therefore tested whether a highly quantitative digital scoring platform might improve CTC detection in early disease, and potentially help distinguish between aggressive and indolent localized prostate cancer.

The CTC_M Score described above generates relatively low levels of signal in men with localized prostate cancer (Fig. 2A). We therefore applied a whole transcriptome amplification (WTA) step prior to the droplet digital PCR assay to amplify the CTC transcript signal (Fig. 5A; see Methods). This WTA-based droplet digital prostate assay was applied prospectively to a cohort of 34 men who had a diagnosis of clinically localized prostate cancer and who were scheduled for radical prostatectomy (Suppl. Table S4). Of these 34 patients, 13 (38%) had a pre-operative prostate biopsy revealing Gleason score 6 (Grade Group 1) disease, 15 (44%) had Gleason score 7 (Grade Group 2 or 3) disease, and 6 (18%) had a Gleason score of 8 or higher (Grade Group 4 or 5). None of these patients had

evidence of seminal vesicle invasion or lymph node metastases on standard pre-operative radiographic imaging, thereby making them candidates for surgical resection (79.4% of patients had a pelvic MRI or abdomen and pelvis CT scan; Suppl. Table. S4). However, following radical prostatectomy, 6 patients (18%) were found on pathologic examination of the resected surgical specimen to have evidence of seminal vesicle invasion (SVI), pelvic lymph node involvement (LN), or a combination of both features, signifying microscopic dissemination of cancer outside the prostate gland (Suppl. Table. S4). Notably, pre-operative digital CTC signal was highly associated with pathological evidence of early prostate cancer dissemination. Elevated expression of several individual genes within the prostate CTC assay gene panel was significantly associated with SVI (FAT1, FOLH1, KLK2, KLK3, and TMPRSS2) and LN involvement (FAT1, FOLH1, KLK2, KLK3, HOXB13, and TMPRSS2) (Suppl. Figs. S5B and S5C).

We developed a weighted CTC score for early dissemination in localized prostate cancer (CTC_L Score) using differential weighting of individual genes based on their predictive value for SVI or LN involvement (Fig. 5B; Suppl. Fig. S5B). A pre-operative CTC_L Score higher than two standard deviations above the average healthy donor signal was strongly associated with pathologic SVI or LN involvement discovered at the time of radical prostatectomy (Fig. 5C; $P<0.001$). This association remained significant even after performing a leave-one-out cross validation with the complete radical prostatectomy data set (Suppl. Fig. S6A; see Methods). A leave-one-out cross validated (LOOCV) CTC_L Score in localized prostate cancer was not significantly correlated with biopsy Gleason score (Suppl. Fig. S6B), Grade Group (Suppl. Fig. S6C), or preoperative serum PSA (Suppl. Fig. S6D). Comparison of the LOOCV CTC_L Score and standard clinicopathologic risk groupings showed that the CTC_L Score had superior predictive value in this cohort with respect to prediction of pathologic SVI or LN involvement (Figs. 5D, 5E, and 5F). For patients with a high CTC_L Score, the positive predictive value (PPV) for SVI or LN invasion was 100% (3/3 patients), compared to a PPV of 33% (3/9) for patients with a high score in the commonly used D'Amico clinical risk group (18) (Fig. 5D and5F), and a PPV of 60% (3/5) in the UCSF CAPRA Score (21) (Fig. 5E and 5F). The negative predictive value (NPV) was similar for all three measures (90% for CTC_L Score, 88% for D'Amico, and 90% for CAPRA) (Fig. 5F). The use of combinations of the CTC_L Score together with either CAPRA or D'Amico risk groupings did not appreciably increase the PPV or NPV for pre-operative prediction of SVI or LN involvement (Fig. 5F). Despite the small sample size, these observations raise the possibility that digital CTC analyses may help predict the presence or absence of early dissemination in patients undergoing surgical resection for a presumed localized prostate cancer.

Discussion

By combining microfluidic enrichment of unfixed CTCs with digital quantitation of CTC-derived RNA, we describe a highly sensitive and specific assay for non-invasive sampling of prostate cancer. The digital RNA-based scoring overcomes several limitations of cell imaging-based CTC analyses, including the requirement for calibration and thresholding of multiple immuno-fluorescence microscopy parameters and manual verification of individual images. In addition, the high sensitivity and specificity of sequence-based approaches, which

are readily multiplexed to simultaneously interrogate multiple markers, provide greatly improved signal over traditional cell imaging methods. We demonstrate potential applications of this digital CTC assay in the settings of both metastatic and clinically localized prostate cancer (Fig. 6). In a prospective study of men on first-line abiraterone therapy for mCRPC, quantitative digital CTC measurements of both normal prostatic transcripts and aberrant RNA products identify a patient subset that is poorly responsive to AR-targeted therapy. In a second study of men undergoing radical prostatectomy for localized prostate cancer, digital CTC analysis predicts for the presence of clinically significant cancer dissemination that is not detected by standard preoperative clinical imaging and could impact the choice of curative intervention.

Conceptually, the application of a digital RNA-based PCR output to microfluidic CTC-enriched cell populations presents several important advantages. First, the use of purified whole CTCs in the bloodstream as the source of RNA increases the likelihood that the measured signal is derived from invasive cancer cells, as opposed to normal tissues or indolent cancers. Second, the analysis of cancer cells within a background of normal blood cells enables the use of tissue lineage-based RNA transcripts that are not unique to cancer, thereby expanding the number of available biomarkers and confirming the tissue-of-origin for these circulating cancer cells. Third, lineage RNA-based CTC measurements may be applied to virtually all prostate cancers, without the need to develop individualized genotype assays based on primary tumor sequencing, nor do they rely on the presence of recurrent cancer-specific mutations, which are relatively infrequent in prostate cancer (35).

In addition to prostate lineage-based RNA markers, aberrant AR mRNA splice variant and TMPRSS2-ERG translocation transcript expression provide a high degree of specificity for prostate cancer, and they also require the use of RNA measurements in blood-based analyses. In this context, the microfluidic depletion of normal hematopoietic cells from blood specimens is particularly effective in preserving RNA integrity within CTCs, which are not subject to antibody-manipulation or fixation and thus provide excellent signal for digital PCR quantitation. Along with microfluidic CTC isolation, digital scoring of CTC signal for both prostate lineage transcripts and prostate cancer-specific transcripts can be readily automated for high-throughput analyses, making it a practical tool for clinical applications.

The recent development of multiple potent treatment modalities for metastatic prostate cancer brings with it the need to identify predictive biomarkers of response (1). To date, the most significant markers have focused on the demonstration of continued activity of the androgen receptor, which is targeted by many therapies for mCPRC. Molecular imaging-based strategies to measure androgen signaling have been demonstrated in some cases, but the availability of blood-based sampling would greatly enhance the utility of such monitoring (36). We have previously reported that scoring of CTCs for expression of the androgen-driven protein PSA versus the androgen-repressed protein PSMA can be translated into an “AR-on” versus “AR-off” CTC immunofluorescence-based signature (9). In treatment-naive patients, virtually all CTCs have “AR-on” signal, which converts to “AR-off” following initiation of androgen depletion therapy (ADT). Patients with mCRPC, however, frequently show simultaneous expression of “AR-on” and “AR-off” protein

signatures, consistent with aberrant AR signaling. In this context, the predictive value of CTC-derived *HOXB13* mRNA is of particular interest. *HOXB13* is a lineage-specific modulator of AR transcriptional activity, which has been shown to interact with AR and reprogram the AR cistrome during prostate tumorigenesis (37). *HOXB13* is normally repressed by AR signaling, hence its abundance in CTCs from men with mCRPC is consistent with aberrant AR signaling. Of note, germline mutations in *HOXB13* have been correlated with increased susceptibility to prostate cancer (38). Taken together, overexpression of *HOXB13* within prostate CTCs may identify cancers in which altered AR signaling pathways contribute to disease progression, thereby lessening the effectiveness of abiraterone and other AR-targeted therapies.

AR-V7 has recently emerged as a readily measurable biomarker for acquired androgen pathway independence, predicting resistance to abiraterone or enzalutamide therapy (12, 13). Discordant results as to the predictive value of ARV7 measurements most likely result from different CTC or exosome-based detection assays (39), as well as their application in patients at different stages of treatment and disease progression. For instance, in large retrospective clinical trials, AR-V7 was detectable in CTCs from only 3% of patients prior to second line therapy using an immunofluorescence assay (13), and in 12.1% of patients using qRT-PCR (14). While our prospective cohort was relatively small, the application of a sensitive and quantitative digital CTC assay in patients who are relatively early in their disease course provides a novel perspective on the significance of AR-V7 positivity. First, we note that detection of this splice variant in mCRPC patients in the first-line setting does not by itself indicate resistance to abiraterone; however, the elevation of CTC AR-V7 transcript levels above a specific threshold is highly predictive of adverse outcome. Single cell RNA sequencing has demonstrated considerable heterogeneity among AR splice variants even among CTCs from the same individual (11), hence the quantitative scoring provided by digital PCR analysis may provide a robust and standardized platform. Second, the observation that downstream indicators of altered AR signaling (e.g. *HOXB13*) are more commonly elevated than AR-V7 and are more predictive of adverse outcome suggests that AR-V7 is only one of a number of markers that predict reduced efficacy of AR targeted therapies. Larger prospective clinical trials of both prostate lineage-markers and AR-V7 will be required to extend these findings and define the relative utility of monitoring CTC-derived markers in guiding therapy with abiraterone and other AR-targeted therapies. The recent application of combined therapies in the initial treatment of high risk metastatic prostate cancer, including the combination of docetaxel and ADT (40) and the combination of abiraterone and ADT (41), raise the possibility that risk stratification may also enable individualized therapies in advanced disease.

Finally, using whole transcriptome amplification to enhance signal, we tested the potential application of digital CTC Scoring in the evaluation of clinically localized prostate cancer. In this context, the primary challenge is accurate risk stratification to guide the reduction in therapeutic interventions in cases at lower risk, while providing more aggressive treatment of high risk disease. Standard risk stratification tools and nomograms, based on clinical staging and prostate core biopsies, are often unreliable in predicting the microscopic extent of disease identified at the time of surgery, likely due in part to the limited sampling of the prostate at the time of diagnostic biopsy (22, 23). In the cohort described here, patients with

high pre-operative CTC_L Scores were subsequently found at the time of radical prostatectomy to have a high rate of seminal vesicle invasion or pelvic lymph node involvement. These findings were not predicted by histopathologic analysis of the diagnostic biopsies, by preoperative serum PSA level, or by clinical or radiographic staging. As expected, the frequency of microscopic dissemination discovered at the time of surgery was low (6/34 cases; 18%), but these findings may have important clinical consequences, and all six cases were referred for consideration of postoperative radiation therapy and/or androgen deprivation therapy, thereby incurring the potential for additional treatment-related adverse events. Additional clinical follow-up of our cohort is necessary to determine if the pre-operative CTC_L Score correlates with biochemical recurrence and other prostate cancer-specific outcomes. If confirmed in larger studies, the high predictive value of the CTC_L Score for microscopic dissemination of early prostate cancer may provide a biomarker to help identify high risk patients who may benefit from alternative treatment approaches, including neoadjuvant preoperative systemic therapies, or radiation therapy in combination with novel systemic therapies. In addition, while this study involved single CTC measurements performed preoperatively and standardized against separate control cohorts, serial longitudinal monitoring of the CTC_L Score may ultimately allow individualization of the baseline signal for each patient, with potential applications in monitoring men with indolent prostate cancers undergoing active surveillance for early indication of disease progression. Thus, RNA-based digital CTC scoring provides a highly sensitive and quantitative blood-based marker to complement standard clinical parameters, with the goal of optimizing treatment algorithms in both early and advanced prostate cancer.

Materials and Methods

Patients and clinical specimens

All studies were conducted in accordance with Belmont Report ethical guidelines. Patients with a diagnosis of prostate cancer provided informed written consent to one of two Institutional Review Board (IRB) approved protocols, DF/HCC 05–300 or DF/HCC 13–209. A total of 88 patients donated 20 mL of blood for CTC analysis, including 46 patients with metastatic prostate cancer and 42 patients with localized prostate cancer (see Suppl. Tables S2, S3, and S4). Patients with mCRPC starting abiraterone included the first 27 evaluable subjects of an ongoing, single-arm, 40-patient, investigator-initiated pilot study evaluating CTCs in patients receiving abiraterone at standard dosing (see Suppl. Table S3; ClinicalTrials.gov NCT01961843). Subjects were required to have mCRPC, rising PSA >2ng/dL, good overall performance status, and adequate organ function. Subjects signed informed consent. The study drug was supplied by Janssen LLC; all data collection and interpretation were performed by the authors. The complete clinical and CTC evaluation from the study will be reported separately upon completion of the study. Disease status and therapy at the time of CTC collection for each of the metastatic patients are provided in Suppl. Tables S2 and S3. For a subset of these patients, matched archival formalin-fixed, paraffin-embedded (FFPE) primary tumor tissues were sectioned, macrodissected for >70% tumor content, and subjected to RNA extraction, prior to processing for droplet digital PCR (see below).

For testing of the CTC_L Score, 34 patients with clinically localized prostate cancer who were scheduled to undergo radical prostatectomy donated 20mL of blood prior to surgery. Detailed clinical and pathologic characteristics for these localized prostate cancer patients are provided in Suppl. Table S4.

Circulating tum or cell isolation

CTCs were isolated from fresh whole blood donated by patients or healthy donors following leukocyte depletion using the microfluidic CTC-iChip as previously described. To maximize recovery of intact CTCs with high quality RNA, blood samples were processed within 4 hours of being collected from the patient. The total time for CTC isolation after receipt of fresh blood samples in the lab was approximately 2.5 hours. Briefly, whole blood samples were spiked with biotinylated antibodies against CD45 (R&D Systems, clone 2D1) CD66b (AbD Serotec, clone 80H3), and CD16 (Janssen Diagnostics), followed by incubation with Dynabeads MyOne Streptavidin T1 (Invitrogen) to achieve magnetic labeling and depletion of white blood cells. After processing of whole blood with the CTC-iChip and collecting the enriched CTC product on ice, cells were centrifuged at 4750 rpm and flash frozen in liquid nitrogen in the presence of *RNAlater*® (Ambion) to preserve RNA integrity.

RNA extractions, cDNA synthesis, and whole transcriptom e amplification (WTA)

CTC samples were subjected to RNA extraction using the RNeasy Plus Micro Kit (Qiagen). FFPE primary prostate tumor tissues were subjected to RNA extraction using the Allprep DNA/RNA FFPE kit (Qiagen), using xylene deparaffinization and a 16 hour incubation in proteinase K solution at 56°C prior to RNA extraction. Complementary DNA (cDNA) was prepared from purified RNA using SuperScript III First-Strand Synthesis System (Life Technologies). Whole transcriptome amplification (WTA) was performed on RNA using the SMARTer Ultra Low-input RNA kit, version 4 (Clontech Laboratory).

Cell Culture and Cell Line Spiking Experim ents

LNCaP (2009), VCaP (2010), and 22Rv1 (2013) cells were obtained from American Type Culture Collection (ATCC) in the years indicated, and grown in the recommended medium. All cell lines were authenticated by Short Tandem Repeat profiling and tested negative for Mycoplasma on a yearly basis, most recently in August 2016 for experiments in this Article. Cells were used in all experiments within 15 to 20 passages from thawing. To test the limit of detection for the ddPCR assay, cell spiking experiments were performed as follows. Single prostate cancer cell line cells were manually manipulated using 10um Eppendorf TransferMan NK2 transfer tips into Kolliphor P188 buffer and spiked under direct microscopic visualization (Nikon Eclipse Ti-U inverted microscope) into 4 mL aliquots of healthy donor male blood. The spiked samples were then processing using the CTC-iChip as described above.

Droplet Digital PCR

cDNA and primer/probe mixes were combined with ddPCR Supermix for Probes (Bio-Rad) in a 96-well plate and loaded onto Bio-Rad's automated droplet generator. Droplets were subjected to thermal cycling using a modified 45-cycle PCR with a 70°C step-down in

between the denaturation and annealing steps. Following thermal cycling, droplets containing the transcript of interest were detected via fluorescence with the QX200 Droplet Reader System (Bio-Rad). In general, droplet digital PCR assays for CTCs isolated from patients with metastatic prostate cancer were performed without a preamplification step, with the exception of the TMPRSS2:ERG assay, for which a 14-cycle specific targeted amplification (STA) was performed using TaqMan PreAmp Master Mix (Invitrogen) prior to droplet digital PCR using a separate set of nested primers (see below) to increase the sensitivity of the assay. To analyze CTCs from patients with localized prostate cancer (for the CTC_L-Score), WTA was performed to amplify the RNA prior to subjecting to ddPCR.

Droplet Digital PCR Primers

A list of potential gene candidates for the prostate CTC ddPCR assay was generated using publically available databases as well as single cell RNA-seq data (see Suppl. Table S1). A multi-step approach using qRT-PCR and ddPCR was developed to test the specificity of ddPCR primers and probes designed to detect these transcripts (Suppl. Fig. S1A). Candidate primers and probes were tested for signal in cancer cell cDNA and absence of signal in leukocyte cDNA using the ABI 7500 and Bio-Rad CFX96 Real-Time PCR Systems.1ng of total cDNA was used per qRT-PCR reaction. Primer/probe combinations for genes that showed signal in cell lines and absence of signal in healthy donor leukocytes by qRT-PCR were further validated using ddPCR. Each primer/probe combination was testing using cDNA prepared from CTC-iChip products of healthy donor males and prostate cancer patients using the ddPCR platform, as above (Bio-Rad). The sequences of the primers and probes used for each gene in the Prostate CTC ddPCR Assay are provided in Suppl. Table S5.

Immunofluorescence and Cell Imaging

Isolated CTCs were subjected to immunofluorescence staining using previously established protocols, with modifications. Briefly, the CTC-iChip product was fixed for 10 minutes in 1% formaldehyde/P188 Kolliphor and plated onto poly-L-lysine coated glass slides (Sigma Aldrich) using a Shandon Cytospin 4 and EZ Megafunnel (Thermo Fisher), centrifuging at 2000 rpm for 5 minutes. The cells were dried for 10 minutes and immunostained with antibodies against CK8/18 (C11, mouse IgG1, Janssen) and CK19 (A53, mouse IgG2a, Jannsen) conjugated to Alexa Fluor 488 (Invitrogen), PSA (D6B1, rabbit IgG, Cell Signaling Technologies), PSMA (J591, mouse IgG, N.H. Bander) conjugated to Alexa Fluor 555 (Invitrogen), CD45 (HI30, mouse IgG1, Biolegend) and CD16 (3G8, mouse IgG1, Biolegend) and CD66b (G10FS, mouse IgG1, Biolegend) conjugated to Alexa Fluor 647 (Invitrogen), followed by goat anti-rabbit secondary antibody conjugated to Alexa Fluor 549 (Invitrogen) and DAPI.

Stained slides were imaged using an automated multispectral imaging microscope (PerkinElmer Vectra 2.0.8) at 20× magnification using DAPI, FITC, Cy3, and Cy5 filters. Vectra and InForm software (PerkinElmer) were used for automated image capture and spectral unmixing into 5 channels. Human validation of candidate CTCs was performed using CellReview software (PerkinElmer), using a minimum signal threshold of 50, 50, and 15 for cytokeratin, PSA, and PSMA markers respectively.

Multi-class Support Vector Machine (SVM) classifier

To generate training and validation sets for the multi-class support vector machine (SVM) classifier, 10 ng of LNCaP cell cDNA was loaded into each ddPCR reaction. By appropriately isolating each probe set combination into separate PCR reactions (individual reactions with probes for only one of the genes of interest, and reactions with probes for only two genes of interest to allow for the unambiguous identification of the resultant double-positive droplets), we could confidently manually curate the FAM/HEX values that corresponded to a given class of single- or double-positive droplet. These data were manually classified using the FlowJo software package and then imported into MATLAB. A custom MATLAB script was used to generate and validate a multi-class support vector machine (SVM) classifier with 30% of the droplets partitioned prior to SVM training and allocated as the testing set. To best match new ddPCR data derived from patient CTCs to the initial LNCaP results used to train the SVM, a user is asked to manually confirm that the four single positive droplets for a given reaction are located within the appropriate area on the FAM/HEX plot. If the user determines that they are not, the user can translate the origin of the data via the MATLAB command line. Raw data files and MATLAB scripts with detailed commenting available upon request.

CTC_M Score

To generate a weighted digital CTC score in metastatic prostate cancer, blood samples were obtained from 34 male healthy donors and 12 patients with metastatic prostate cancer, processed using the iChip, and analyzed using the multiplex droplet digital PCR assay (see Results; Fig. 2A; Suppl. Fig. S2). For each gene *i* in the 8-gene assay, the average number of positive droplets per sample in the 34 male healthy donor samples (HD_i) was compared to the average number of positive droplets per sample in the 12 metastatic prostate cancer patients (MP_i) (Suppl. Fig. S2). The ratio = MP_i/HD_i was calculated for each gene *i*. Using each ratio R_i as a weighting factor for each gene *i*, the CTC score was then derived as follows:

$$CTC_M{}^{score} = \left(\sum_{i=1}^{n} \left(R_i * D_i \right) \right) / 1000$$

where *i* is each gene, *n* is the number of genes assayed, R_i is the weighting factor for each gene *i*, and D_i is the number of positive droplets for gene *i* for any given CTC sample (see Fig. 2B for full equation used in this study).

To determine the optimal division points within the CTC Score and individual genes for overall survival and radiographic progression-free survival within the abiraterone mCRPC cohort, the algorithm of Contal-O'Quigley was applied to the data using leave-one-out jack-knife resampling. Each iteration of the algorithm produced an estimate of the "best" division point based on the data. The mode of the distribution of "best" values was carried forward as the selected cut point for each individual gene. The advantage of using the algorithmic approach is that it is objective and is designed to find the "best" division that the data can provide, unlike splitting at the median or quartiles.

CTC_L Score

All analysis was performed using R version 3.3.1 and the R scripts used are available upon request. Patient data was imported into the R computing environment, and the CAPRA and D'Amico scores calculated as previously described. The CTC_L score was generated by dividing the average number of transcripts for a given gene in the invasive samples by the average number of transcripts for a given gene in the non-invasive sample to generate a gene weight. Next, each gene for a given sample was multiplied by that gene's weight, and the resulting weighted gene counts summed to provide a CTC_L score (Fig. 5B). In order to generate an estimation of this approach's performance on new data, we performed leave-one-out cross-validation (LOOCV) (42); all subsequent claims are based on these LOOCV results. To define a threshold value delineating "CTC_L positive" from "CTC_L negative," we calculated the CTC_L score (using the entire radical prostatectomy patient data to generate gene weights) for a panel of 30 age-matched male healthy donors. CTC_L positivity was defined as the mean healthy donor CTC_L Score plus two times the standard deviation of the healthy donor CTC_L Score. A chi-squared test was performed to determine if CTC_L positivity was associated with invasion (Fig. 5C).

Statistical Analyses

Overall survival was defined as the interval between the start of therapy and the date of death or censor. Radiographic progression-free survival was defined as the interval between the start of therapy and the date of radiographic progression, death, or censor. Survival curves were generated using the Kaplan-Meier method and compared using the log-rank test. Two-sided *P*-values <0.05 were considered statistically significant. Statistical analyses were performed using R, version 3.3.1.

Supplementary Material

Refer to Web version on PubMed Central for supplementary material.

Acknowledgements

We thank Janssen for clinical trial support, C. Gurski for clinical research support, and L. Libby and L. Nieman for technical assistance. This work was supported by awards from the Prostate Cancer Foundation (D.T.M., D.A.H., S.M., M.R.S., R.J.L.), Charles Evans Foundation (D.A.H.), Department of Defense (D.T.M.), Howard Hughes Medical Institute (D.A.H.), National Institute of Biomedical Imaging and Bioengineering (5U01EB012493) (M.T. and D.A.H.), National Institute of General Medical Sciences (T32GM007753) (M.K.), Burroughs Wellcome Fund (D.T.T.), and the MGH-Johnson & Johnson Center for Excellence in CTC Technologies (M.T., S.M.). MGH and the authors have applied for patent protection for the CTC-iChip technology and molecular signatures.

References

1. Scher HI, Morris MJ, Larson S, Heller G. Validation and clinical utility of prostate cancer biomarkers. Nat Rev Clin Oncol 2013; 10: 225–34. [PubMed: 23459624]
2. Armstrong AJ, Eisenberger MA, Halabi S, Oudard S, Nanus DM, Petrylak DP, et al. Biomarkers in the management and treatment of men with metastatic castration-resistant prostate cancer. Eur Urol 2012; 61: 549–59. [PubMed: 22099611]
3. Scher HI, Morris MJ, Stadler WM, Higano C, Basch E, Fizazi K, et al. Trial Design and Objectives for Castration-Resistant Prostate Cancer: Updated Recommendations From the Prostate Cancer Clinical Trials Working Group 3. J Clin Oncol 2016; 34:1402–18. [PubMed: 26903579]

4. Gillessen S, Omlin A, Attard G, de Bono JS, Efstathiou E, Fizazi K, et al. Management of patients with advanced prostate cancer: recommendations of the St Gallen Advanced Prostate Cancer Consensus Conference (APCCC) 2015. Ann Oncol 2015; 26: 1589–604. [PubMed: 26041764]
5. Mateo J, Carreira S, Sandhu S, Miranda S, Mossop H, Perez-Lopez R, et al. DNA-Repair Defects and Olaparib in Metastatic Prostate Cancer. N Engl J Med 2015; 373: 1697–708. [PubMed: 26510020]
6. Scher HI, Heller G, Molina A, Attard G, Danila DC, Jia X, et al. Circulating tumor cell biomarker panel as an individual-level surrogate for survival in metastatic castration-resistant prostate cancer. J Clin Oncol 2015; 33:1348–55. [PubMed: 25800753]
7. Miyamoto DT, Sequist LV, Lee RJ. Circulating tumour cells-monitoring treatment response in prostate cancer. Nat Rev Clin Oncol 2014; 11: 401–12. [PubMed: 24821215]
8. Watson PA, Arora VK, Sawyers CL. Emerging mechanisms of resistance to androgen receptor inhibitors in prostate cancer. Nat Rev Cancer 2015; 15: 701–11. [PubMed: 26563462]
9. Miyamoto DT, Lee RJ, Stott SL, Ting DT, Wittner BS, Ulman M, et al. Androgen receptor signaling in circulating tumor cells as a marker of hormonally responsive prostate cancer. Cancer Discov 2012; 2: 995–1003. [PubMed: 23093251]
10. Lu C, Luo J. Decoding the Androgen Receptor Splice Variants. Transl Androl Urol 2013; 2: 178–86. [PubMed: 25356377]
11. Miyamoto DT, Zheng Y, Wittner BS, Lee RJ, Zhu H, Broderick KT, et al. RNA-Seq of single prostate CTCs implicates noncanonical Wnt signaling in antiandrogen resistance. Science 2015; 349: 1351–6. [PubMed: 26383955]
12. Antonarakis ES, Lu C, Wang H, Luber B, Nakazawa M, Roeser JC, et al. AR-V7 and Resistance to Enzalutamide and Abiraterone in Prostate Cancer. N Engl J Med 2014.
13. Scher HI, Lu D, Schreiber NA, Louw J, Graf RP, Vargas HA, et al. Association of AR-V7 on Circulating Tumor Cells as a Treatment-Specific Biomarker With Outcomes and Survival in Castration-Resistant Prostate Cancer. JAMA Oncol 2016.
14. Antonarakis ES, Lu C, Luber B, Wang H, Chen Y, Zhu Y, et al. Clinical Significance of Androgen Receptor Splice Variant-7 mRNA Detection in Circulating Tumor Cells of Men With Metastatic Castration-Resistant Prostate Cancer Treated With First- and Second-Line Abiraterone and Enzalutamide. J Clin Oncol 2017; 35: 2149–56. [PubMed: 28384066]
15. Arora VK, Schenkein E, Murali R, Subudhi SK, Wongvipat J, Balbas MD, et al. Glucocorticoid receptor confers resistance to antiandrogens by bypassing androgen receptor blockade. Cell 2013; 155: 1309–22. [PubMed: 24315100]
16. Beltran H, Prandi D, Mosquera JM, Benelli M, Puca L, Cyrta J, et al. Divergent clonal evolution of castration-resistant neuroendocrine prostate cancer. Nat Med 2016; 22: 298–305. [PubMed: 26855148]
17. Hamdy FC, Donovan JL, Lane JA, Mason M, Metcalfe C, Holding P, et al. 10-Year Outcomes after Monitoring, Surgery, or Radiotherapy for Localized Prostate Cancer. N Engl J Med 2016; 375: 1415–24. [PubMed: 27626136]
18. D'Amico AV, Whittington R, Malkowicz SB, Schultz D, Blank K, Broderick GA, et al. Biochemical outcome after radical prostatectomy, external beam radiation therapy, or interstitial radiation therapy for clinically localized prostate cancer. JAMA 1998; 280: 969–74. [PubMed: 9749478]
19. Partin AW, Mangold LA, Lamm DM, Walsh PC, Epstein JI, Pearson JD. Contemporary update of prostate cancer staging nomograms (Partin Tables) for the new millennium. Urology 2001; 58: 843–8. [PubMed: 11744442]
20. Kattan MW, Eastham JA, Stapleton AM, Wheeler TM, Scardino PT. A preoperative nomogram for disease recurrence following radical prostatectomy for prostate cancer. J Natl Cancer Inst 1998; 90: 766–71. [PubMed: 9605647]
21. Cooperberg MR, Pasta DJ, Elkin EP, Litwin MS, Latini DM, Du Chane J, et al. The University of California, San Francisco Cancer of the Prostate Risk Assessment score: a straightforward and reliable preoperative predictor of disease recurrence after radical prostatectomy. J Urol 2005; 173: 1938–42. [PubMed: 15879786]

22. Dinh KT, Mahal BA, Ziehr DR, Muralidhar V, Chen YW, Viswanathan VB, et al. Incidence and Predictors of Upgrading and Up Staging among 10,000 Contemporary Patients with Low Risk Prostate Cancer. J Urol 2015; 194: 343–9. [PubMed: 25681290]

23. Caster JM, Falchook AD, Hendrix LH, Chen RC. Risk of Pathologic Upgrading or Locally Advanced Disease in Early Prostate Cancer Patients Based on Biopsy Gleason Score and PSA: A Population-Based Study of Modern Patients. Int J Radiat Oncol Biol Phys 2015; 92: 244–51. [PubMed: 25841621]

24. Stott SL, Lee RJ, Nagrath S, Yu M, Miyamoto DT, Ulkus L, et al. Isolation and characterization of circulating tumor cells from patients with localized and metastatic prostate cancer. Sci Transl Med 2010; 2: 25ra3.

25. Davis JW, Nakanishi H, Kumar VS, Bhadkamkar VA, McCormack R, Fritsche HA, et al. Circulating tumor cells in peripheral blood samples from patients with increased serum prostate specific antigen: initial results in early prostate cancer. J Urol 2008; 179: 2187–91; [PubMed: 18423725]

26. Meyer CP, Pantel K, Tennstedt P, Stroelin P, Schlomm T, Heinzer H, et al. Limited prognostic value of preoperative circulating tumor cells for early biochemical recurrence in patients with localized prostate cancer. Urol Oncol 2016; 34: 235 e11–6.

27. Ozkumur E, Shah AM, Ciciliano JC, Emmink BL, Miyamoto DT, Brachtel E, et al. Inertial focusing for tumor antigen-dependent and -independent sorting of rare circulating tumor cells. Sci Transl Med 2013; 5: 179ra47.

28. Kalinich M, Bhan I, Kwan TT, Miyamoto DT, Javaid S, LiCausi JA, et al. An RNA-based signature enables high specificity detection of circulating tumor cells in hepatocellular carcinoma. Proc Natl Acad Sci U S A 2017; 114: 1123–8. [PubMed: 28096363]

29. Hindson CM, Chevillet JR, Briggs HA, Gallichotte EN, Ruf IK, Hindson BJ, et al. Absolute quantification by droplet digital PCR versus analog real-time PCR. Nat Methods 2013; 10: 1003–5. [PubMed: 23995387]

30. Kumar-Sinha C, Kalyana-Sundaram S, Chinnaiyan AM. Landscape of gene fusions in epithelial cancers: seq and ye shall find. Genome Med 2015; 7: 129. [PubMed: 26684754]

31. Saylor PJ, Lee RJ, Arora KS, Deshpande V, Hu R, Olivier K, et al. Branched chain RNA in situ hybridization for androgen receptor splice variant AR-V7 as a prognostic biomarker for metastatic castration-sensitive prostate cancer. Clin Cancer Res 2016.

32. Ryan CJ, Smith MR, de Bono JS, Molina A, Logothetis CJ, de Souza P, et al. Abiraterone in metastatic prostate cancer without previous chemotherapy. N Engl J Med 2013; 368: 138–48. [PubMed: 23228172]

33. de Bono JS, Scher HI, Montgomery RB, Parker C, Miller MC, Tissing H, et al. Circulating tumor cells predict survival benefit from treatment in metastatic castration-resistant prostate cancer. Clin Cancer Res 2008; 14: 6302–9. [PubMed: 18829513]

34. Loh J, Jovanovic L, Lehman M, Capp A, Pryor D, Harris M, et al. Circulating tumor cell detection in high-risk non-metastatic prostate cancer. J Cancer Res Clin Oncol 2014; 140: 2157–62. [PubMed: 25028119]

35. Cancer Genome Atlas Research N. The Molecular Taxonomy of Primary Prostate Cancer. Cell 2015; 163: 1011–25. [PubMed: 26544944]

36. Evans MJ, Smith-Jones PM, Wongvipat J, Navarro V, Kim S, Bander NH, et al. Noninvasive measurement of androgen receptor signaling with a positron-emitting radiopharmaceutical that targets prostate-specific membrane antigen. Proc Natl Acad Sci USA 2011; 108: 9578–82. [PubMed: 21606347]

37. Pomerantz MM, Li F, Takeda DY, Lenci R, Chonkar A, Chabot M, et al. The androgen receptor cistrome is extensively reprogrammed in human prostate tumorigenesis. Nat Genet 2015; 47: 1346–51. [PubMed: 26457646]

38. Ewing CM, Ray AM, Lange EM, Zuhlke KA, Robbins CM, Tembe WD, et al. Germline mutations in HOXB13 and prostate-cancer risk. N Engl J Med 2012; 366: 141–9. [PubMed: 22236224]

39. Bernemann C, Schnoeller TJ, Luedeke M, Steinestel K, Boegemann M, Schrader AJ, et al. Expression of AR-V7 in Circulating Tumour Cells Does Not Preclude Response to Next

Generation Androgen Deprivation Therapy in Patients with Castration Resistant Prostate Cancer. Eur Urol 2016.

40. Sweeney CJ, Chen YH, Carducci M, Liu G, Jarrard DF, Eisenberger M, et al. Chemohormonal Therapy in Metastatic Hormone-Sensitive Prostate Cancer. N Engl J Med 2015; 373: 737–46. [PubMed: 26244877]
41. James ND, de Bono JS, Spears MR, Clarke NW, Mason MD, Dearnaley DP, et al. Abiraterone for Prostate Cancer Not Previously Treated with Hormone Therapy. N Engl J Med 2017; 377: 338–51. [PubMed: 28578639]
42. Hastie T, Tibshirani R, Friedman J. The Elements of Statistical Learning. New York, NY, USA: Springer New York Inc.; 2001.

Statement of Significance

There is an unmet need for biomarkers to guide prostate cancer therapies, for curative treatment of localized cancer and for application of molecularly-targeted agents in metastatic disease. Digital quantitation of prostate CTC-derived transcripts in blood specimens is predictive of abiraterone response in metastatic cancer and of early dissemination in localized cancer.

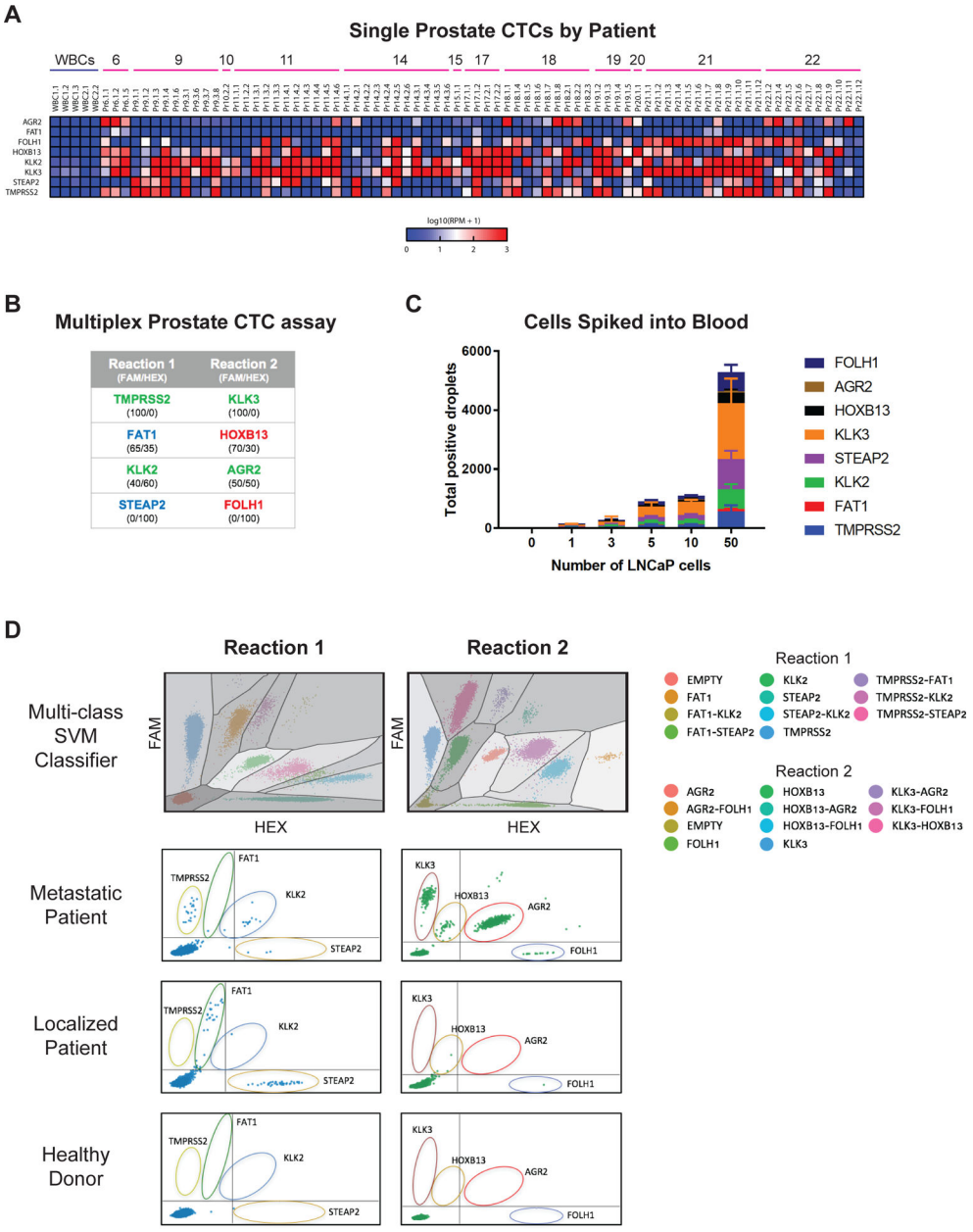

Figure 1.

(A) Single cell RNA-seq data showing expression of final selected genes in WBCs and single prostate CTCs isolated from patients with metastatic prostate cancer (data from GEO GSE67980). **(B)** List of genes contained within each multiplex prostate CTC assay, with FAM/HEX ratio for each probe listed below. Genes in green font are androgen-responsive, genes in red font are androgen-repressed, and genes in blue font are androgen-independent. **(C)** Graph of d-CTC assay signal for varying numbers of LNCaP cells micromanipulated into healthy donor whole blood and processed using the CTC-iChip. **(D)** Top panel: multi-class support vector machine (SVM) classifier model to automatically classify positive droplet signals. Lower 3 panels: representative multiplex ddPCR expression signal in CTCs

from a metastatic prostate cancer patient, a localized prostate cancer patient, and a healthy donor.

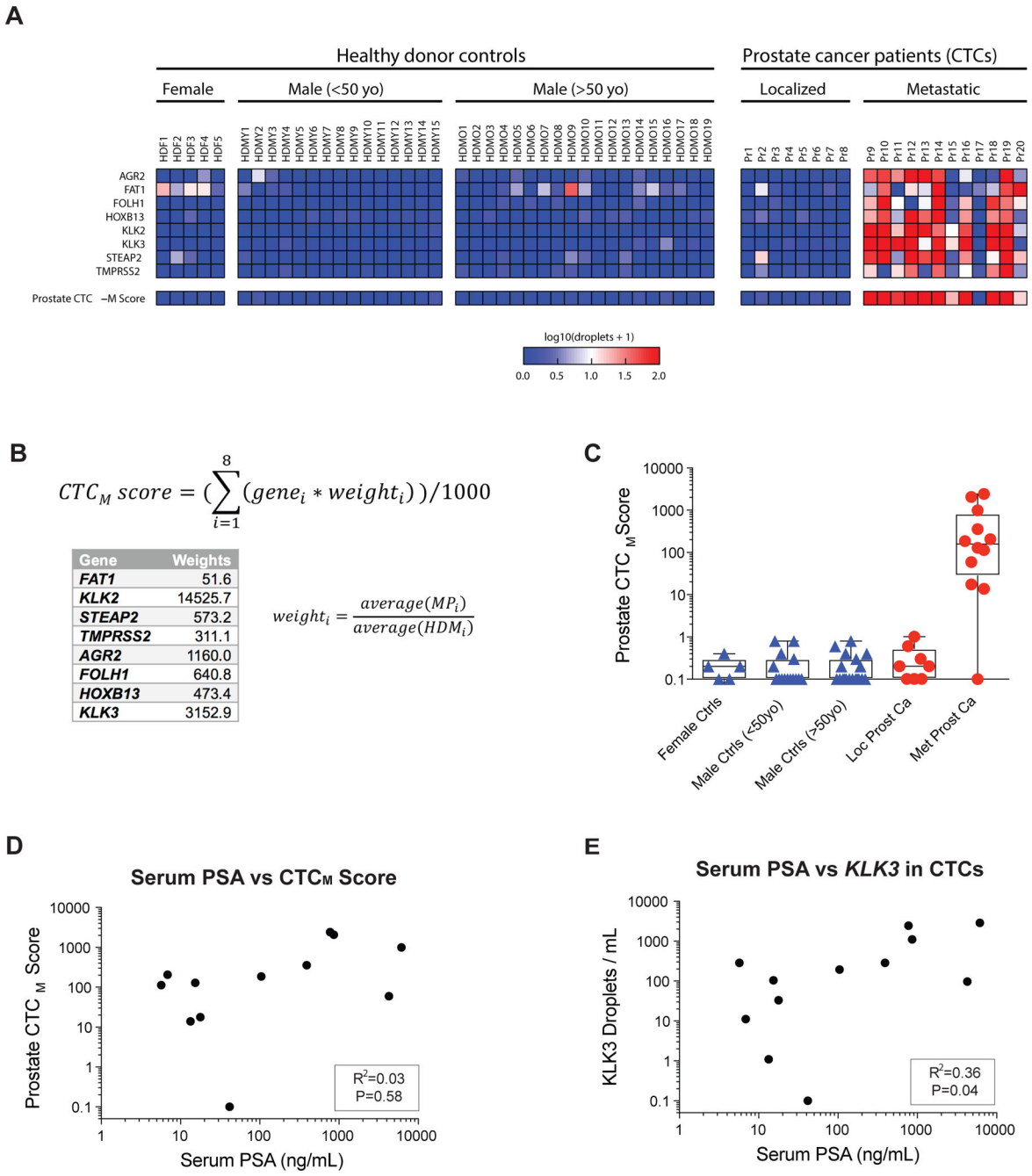

Gene	Weights
FAT1	51.6
KLK2	14525.7
STEAP2	573.2
TMPRSS2	311.1
AGR2	1160.0
FOLH1	640.8
HOXB13	473.4
KLK3	3152.9

Figure 2.

(A) Heatmap showing d-CTC assay signal for each gene in blood obtained from healthy donor controls, localized prostate cancer patients, and metastatic prostate cancer patients. **(B)** Equation for prostate CTC_M Score, with weights for each gene based on the relative signal-to-noise ratio in metastatic patients relative to healthy donors (see Methods). **(C)** Graph showing the quantitation of CTC_M Score signal after application of the prostate CTC_M Score in healthy donor controls, localized prostate cancer patients, and metastatic prostate cancer patients (metastatic patient without signal is Pr17). **(D, E)** Graphs of

relationships between Prostate CTC Score and serum PSA, and CTC droplet digital PCR KLK3 signal and serum PSA in mCRPC patients.

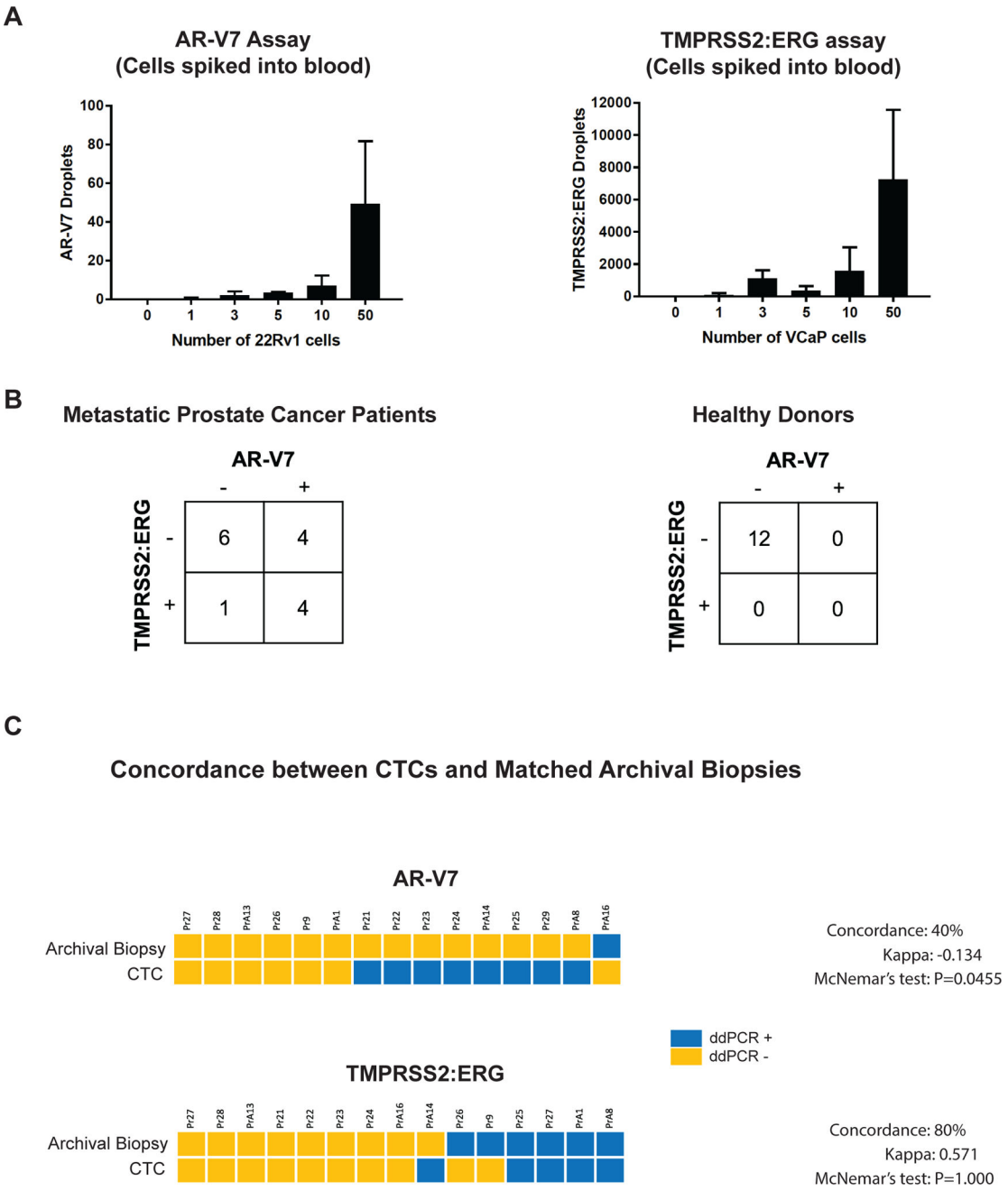

Figure 3.

(A) Graph of droplet digital PCR signal for AR-V7 (no pre-amplification) and TMPRSS2:ERG (after specific targeted amplification; see Methods) for varying numbers of 22Rv1 cells and VCaP cells, respectively, micromanipulated into healthy donor whole blood and processed using the CTC-iChip. **(B)** Tables showing number of metastatic prostate cancer patients and healthy donors with AR-V7 droplet digital PCR signal and/or TMPRSS2:ERG ddPCR signal.**(C)** Concordance of AR-V7 and TMPRSS2:ERG status in prostate CTCs and matched archival FFPE specimens of prostate cancer biopsy or

prostatectomy tissues from prostate cancer patients, as measured by droplet digital PCR assays.

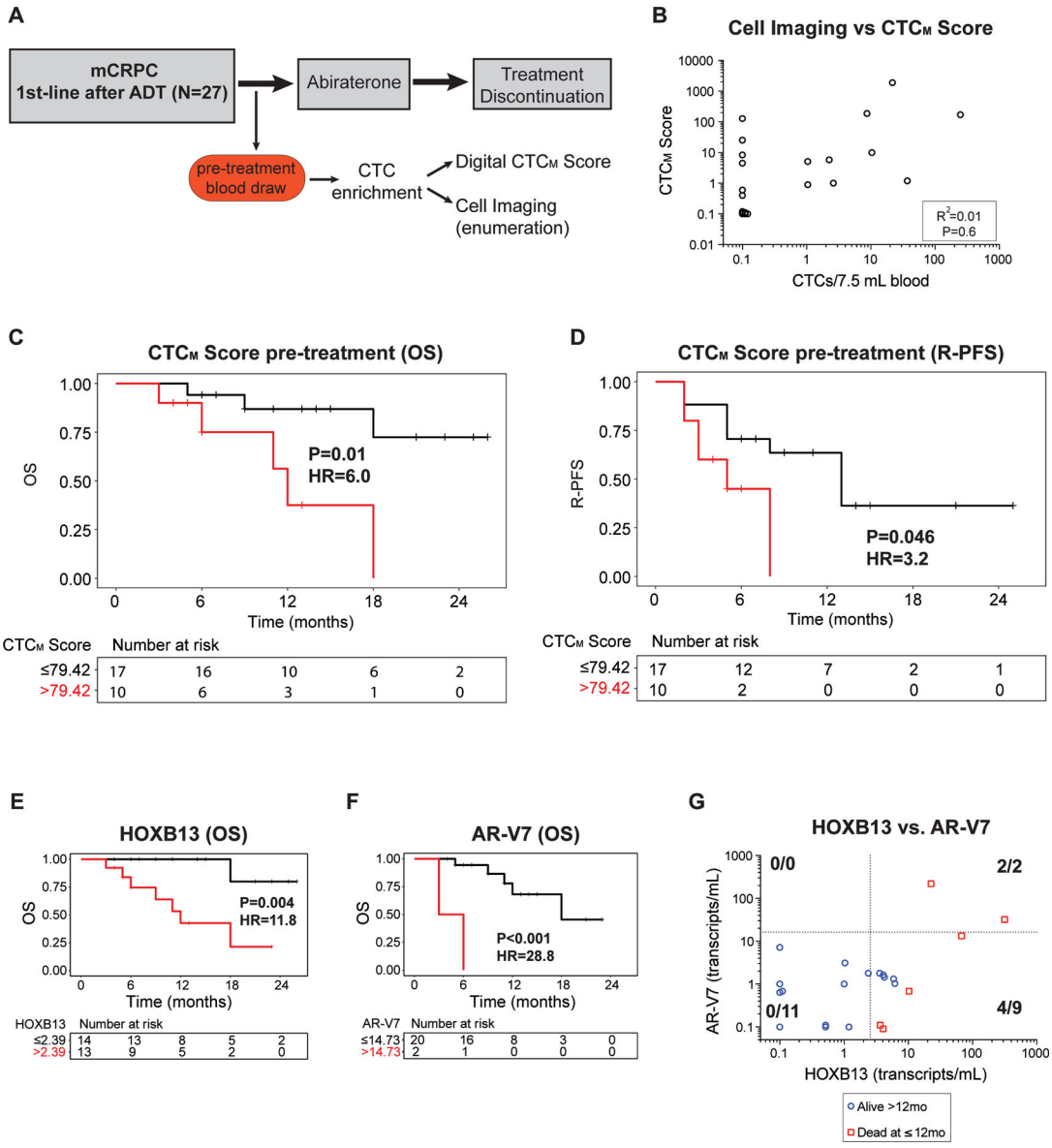

Figure 4.

(A) Schema for prospective study of first-line abiraterone in mCRPC patients, with pre-treatment blood draw followed CTC assessments using digital CTC_M Score and immunofluorescence cell imaging for CTC enumeration. **(B)** Graph of relationship between digital CTC_M Score and CTC enumeration based on cell imaging at the pre-treatment time point. **(C, D)** Kaplan-Meier curves for overall survival (OS) and radiographic progression-free survival (R-PFS) by CTC_M Score at the pretreatment time point. **(E, F)** Kaplan-Meier curves for overall survival (OS) by HOXB13 and AR-V7 CTC signal at the pretreatment time point. 5 patients had pretreatment data available for HOXB13 but not for AR-V7**. (G)** Graph of relationship between HOXB13 and AR-V7 CTC signal (transcripts/mL blood) for CTC samples at the pre-treatment time point for patients for whom data was available for both HOXB13 and AR-V7. Red squares represent patients who died within 12 months of treatment initiation, and blue circles represent those who were alive.

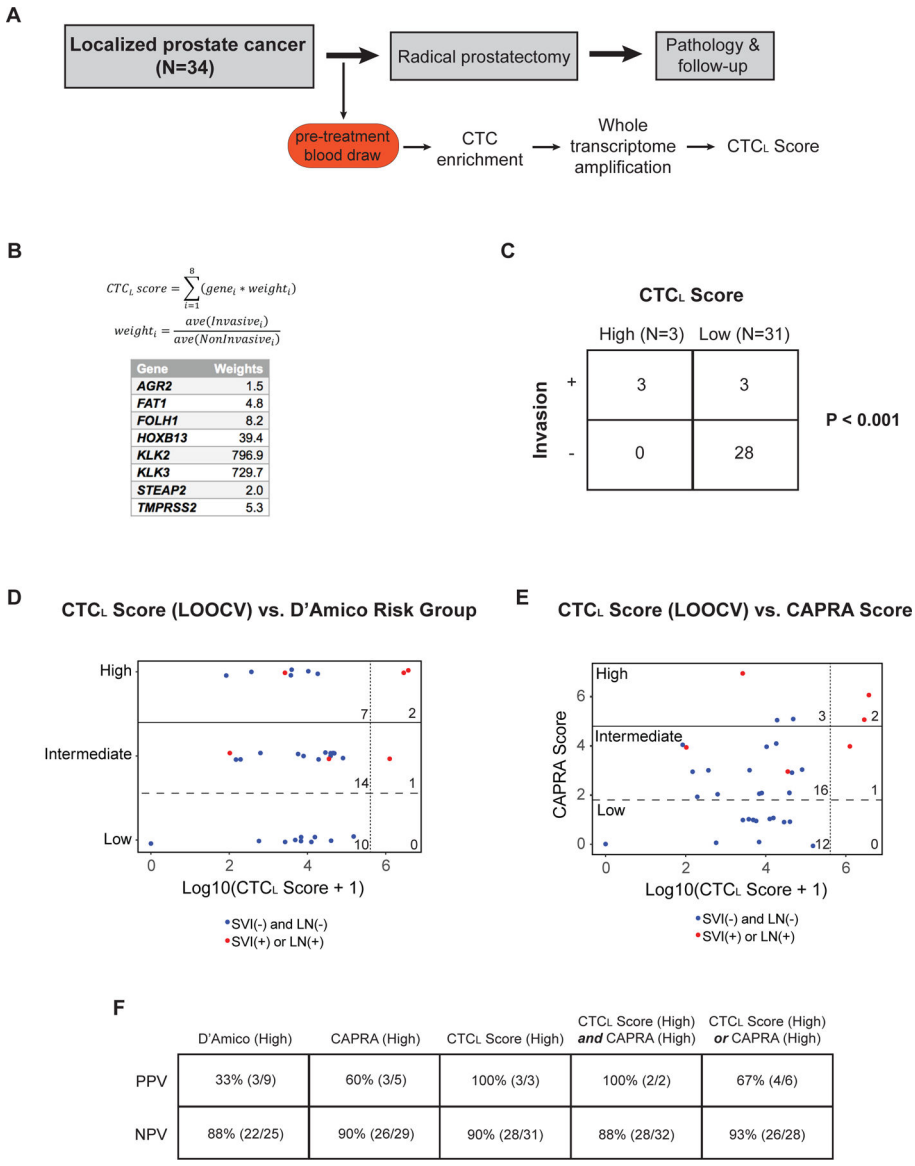

F

	D'Amico (High)	CAPRA (High)	CTCL Score (High)	CTCL Score (High) *and* CAPRA (High)	CTCL Score (High) *or* CAPRA (High)
PPV	33% (3/9)	60% (3/5)	100% (3/3)	100% (2/2)	67% (4/6)
NPV	88% (22/25)	90% (26/29)	90% (28/31)	88% (28/32)	93% (26/28)

Figure 5.

(A) Schema for patients with clinically localized prostate cancer treated with radical prostatectomy in this study. **(B)** Equation for CTC_L Score, with weights for each gene based on the relative signal in localized patients with pathologic seminal vesicle invasion (SVI) or lymph node (LN) involvement, compared to those without microscopic cancer dissemination (see Methods). **(C)** Table showing relationship between the pre-operative CTC_L Score and microscopic SVI or pelvic LN involvement ("Invasion") identified at the time radical prostatectomy. "High" and "Low" CTC_L Scores were determined based on the presence of signal higher than 2 standard deviations above the average signal in healthy donor controls. **(D, E)** Graphs of relationship between pre-operative leave-one-out cross validated (LOOCV) CTC_L Score and D'Amico Risk Group or UCSF CAPRA Score. Red dots represent patients who had microscopic SVI or pelvic LN involvement identified on pathologic examination of the radical prostatectomy specimen, while blue dots represent patients who did not have SVI

or LN involvement. Perpendicular dashed line represents a threshold of 2 standard deviations above the average CTC_L Score signal in healthy donor controls. Numbers depict the number of data points (patients) in each sextant. **(F)** Table showing positive predictive value (PPD) and negative predictive value (PPD) of D'Amico (high risk), CAPRA (high risk), CTC_L Score (high), and CTC_L Score / CAPRA combinations for prediction of microscopic SVI or LN involvement identified at radical prostatectomy.

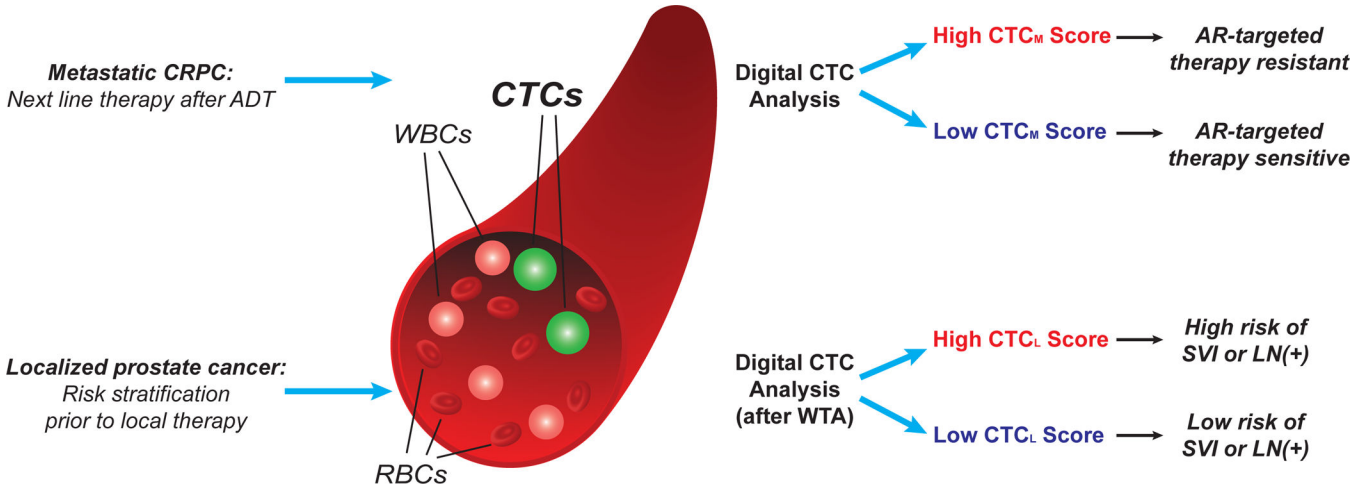

Figure 6.

Schematic showing potential clinical applications of digital CTC analysis in metastatic and localized prostate cancer, including prediction of resistance to AR-targeted therapy in mCRPC (CTC_M Score), and risk of microscopic dissemination to seminal vesicles or lymph nodes in clinically localized prostate cancer (CTC_L Score).